

Published in final edited form as:

IEEE NIH Life Sci Syst Appl Workshop. 2009 May 2; : 36–39. doi:10.1109/LISSA.2009.4906703.

An Image Driven Systems Biology Approach for Neurodegenerative Disease Studies in the TSC-mTOR Pathway

Dominik Beck^{1,2}, Xiaobo Zhou¹, Tuan Pham², Bernardo Sabatini³, and Stephen T.C. Wong¹

¹Center for Biotechnology and Informatics, The Methodist Hospital Research Institute and Department of Radiology, Weill Cornell Medical College, Houston, TX, 77030, U.S.A

²School of Information Technology & Electrical Engineering, The University of New South Wales, Canberra, ACT, 2600, Australia

³Department of Neurobiology, Harvard Medical School, 220 Longwood Ave, Boston, MA 02115, U.S.A

Abstract

In this brief paper we present an overview of the TSC-mTOR pathway and its importance in neurodegenerative disease (ND). We illustrate the influence of ND on dendritic spine morphology. Then we discuss some details of functional gene networks (FGN) and use this information to propose an image driven systems biology approach for the construction of a FGN for ND. We conclude on its importance and the prospective outcome of our study.

I. Introduction

Rapamycin was discovered in 1975 when it was extracted from the soil bacteria *Streptomyces hygroscopicus* [1]. It was categorized as a fungicide and later realized as a strong immunosuppressant. In the early nineties the cellular target of rapamycin was revealed, mainly through systematic studies in yeast and mammals [1-3]. It was named mTOR as the mammalian target of rapamycin. Since that time efforts are high to discover its role in disease, signaling and regulation. In the same decade two other genes were identified from patients suffering from the autosomal dominant tumor syndrome, tuberous sclerosis complex (TSC disease). It was later shown that they function as the major signaling hub towards mTOR. In the last decades a tight pathway around these two components has been established and we illustrate it in Figure 1. It integrates the cell growth related insulin pathway in which IRS, PI3K, PTEN and AKT are major contributors [2]. Another important input is sensing of stress, such as glucose deprivation, hypoxia or muscle concentration. This is mainly detected by AMP and signaled over AMPK. The tumor suppressor gene LKB1 is another important input to AMPK. The pathway also integrates nutrition information over amino acids, and Rheb seems to be one of the main contributors here [4]. The main function is exhibited by mTOR that activates the two molecules S6K and 4EBP1, leading to an enhanced translation capacity and cell growth. More extensive overview about this complex pathway can be found in [3,5,6]. It is responsible for a great variety of human diseases, ranging from benign hematomas to some of the most fatal cancers (indicated in Figure 1). Rapamycin as an inhibitor of mTOR is gaining lots of attention and three homologues, having more favorable pharmacokinetics and solubility properties, are currently in clinical trials, mainly for the treatment of cancer [3,5]. However, in our current work we are particularly interested in ND and discuss the role of the TSC-mTOR pathway in this disease in the next section. In the third section the importance of dendritic spines in ND and their detection through automated imaging is emphasized. The fourth section describes FGN and their application to infer loss of function phenotypes and genes of similar function. The built

information is used through the following section to propose an image guided approach for the construction of a FGN of ND. In the last section we conclude the paper.

II. Gene function analysis of dendritic spines by combined gene knockdowns and image analysis

In our current study we aim to discover a border FGN of ND. We base our approach on the uniting property that many ND, either with or without known TSC-mTOR involvement, affect neurological morphology including dendritic spines and the dendritic tree [7-10]. In most neuronal cells dendritic spines are found along the main shaft, where they provide a micro compartment for segregating postsynaptic chemical responses. They are believed to be the main integrator for postsynaptic excitatory inputs and basically four different shapes exist (thin, stubby, mushroom and cup shaped). In the course of time and due to environmental and molecular factors (overview in [11]) they can change their density, number and different morphological features (e.g. length, size, shape, and the geometry of the spine neck and its length) within minutes or days. A number of morphological variations can be found in human ND, including diseases related to the TSC-mTOR pathway mentioned above and others e.g. ageing or mental retardation [12-18]. These variations, among others, control the activation of glutamate receptors with calcium regulation, cytoskeleton remodeling, membrane trafficking, protein synthesis and degradation, and trans-synaptic signaling [11]. Reviews about dendritic spines, including details of structure, the relation between structure and function, disease and molecular pathways can be found in [7,11,18,19]. The molecular basis and functional effects of different genes on neurons can be studied by gene knockdowns using e.g. RNA interference (RNAi) followed by neuronal imaging. Famous imaging systems in this area include fluorescence life confocal laser scanning or a two-photon laser scanning microscopy [20,21]. After the images are taken they have to be analyzed and morphological changes quantitated. In this manner different groups have studied the effects of different genes on dendritic spine morphology and an overview about some experiments is given in Table 1.

However, since the quantitation part mostly remains a semi-automatic computer based approach it is always subjected to a user dependent bias. Similar to other application, e.g. microarray studies, these user and lab dependent bias makes it very difficult to compare and to integrate such results. Additional this approach is very labor and time intensive. Therefore our group has developed the neuroinformatics application neuron image quantitor (NeuronIQ). This software presents a whole pipeline performing dendritic spine detection, quantification and analysis. It therefore allows for fully automatic and objective image quantification. The software is freely available from our website at neuroniq.cbi-platform.net and an overview about the algorithms, evaluation and further references are given in [21].

III. Integrative gene network construction and interference

In the life sciences many different data types, drawn from a rich pool of experiment, exist and all present different biological or biochemical views. In order to gain the best understanding of the functional dependencies of a certain condition (such as a disease or biological process) one wants to make use of all this information. Integrated FGN try to cover and combine information from all levels into a single probabilistic graph. This is possible as data is integrated by function and thus a link between two genes means that they share similar function. The function criteria allows diverse data types, e.g. pinched from interference (like similar expression profiles) or explicit data (like physical interaction) to be integrated [30]. It is even possible to combine data over different organisms (e.g. using homologues) [31].

In order to construct such a network the first step is to access the quality of each dataset to be included. The quality can be judged against a benchmark, consisting of two gene sets, one including interactions with high confidence and the other interactions with very low confidence [32-34]. These sets can e.g. be based on a GO annotation group or the connections in KEEG [30]. An odds ratio can thus be calculated comparing how well the dataset reflects both gene groups. The odds ratio is normalized against the expected value of a randomly selected gene network. With these quality values the FGN can be constructed. It is represented by a weighted undirected graph $FGN = (V, E)$, where the vertices V represent genes and the edges E represent interactions. Each interaction $(e_i, e_j) \in E$ carries a weight w_{ij} which represents the probability or quality that the connection is really true. Initially edges are set between all nodes that have an interaction in one of the integrated datasets. The weight of an edge is calculated as combination of the normalized odds ratios. In the seldom cases, when the used datasets are statistically independent, a simple sum is adequate for the combination [30]. In all other cases more complex Bayesian statistics or other probabilistic measures have to be used [32-36]. After adjusting the weights the network construction is finished.

It can be validated in the common machine learning framework, e.g. using a cross validation approach comparing the model, or its inference, with datasets not used in its construction (an example based on ROC curves can be found in [34]). Based on the validation a quality level can be assigned.

The inference functionality is however very limited and based merely on its gene connectivity. Therefore, the function of one or ideally many genes is required for inference. If such a set is available, the function of the known genes can be assigned to all its connectives. Furthermore knockdowns of connected genes are likely to result in a similar phenotype. This FGN ability has been shown in yeast [37] and mammalian models [30] where genes with high connectivity show good correlation with loss of function phenotypes. A recent study mentioned that about 20% of the identified genes in a network guided screen effectively suppressed the investigated phenotype [30]. The authors stated that, on contrast, a random wetlab screen is only 0.9% efficient. Thus the approach can be used to guide wetlab experiments, especially in situation with time and financial constraints.

IV. Image based gene network construction for ND

We have discussed that the TSC-mTOR pathway is involved in ND, however its concrete role is not understood yet. A uniting concept between different ND is that they affect the morphology of neurons, including those of dendritic spines. In collaboration with an experimental group we studied the effects of overexpressed and inhibited mTOR on dendritic spines [22]. In the current literature similar experiments for different conditions are reported. Using our software tool NeuronIQ we are able to objectively quantify the morphology of dendritic spines from such images. In combination with the given gene knockdown conditions these features supply us with a wealthy dataset of direct phenotypic features given by

$$F = [f_{m,n}] \quad m=1, \dots, M \quad n=1, \dots, N$$

where M is the number of genes and N the number of image features. We assume that knockdowns of genes sharing a similar function will ultimately lead to similar or the same phenotypic changes. This is much similar to the hypothesis that genes with similar expression under different conditions are assumed to have the same or similar function. However, it represents a different view on the data on a higher level e.g. not prone to

posttranslational modifications. Therefore, we propose that genes with similar function can be inferred from their image features. This can be done by any of the standard pattern classification methods, such as clustering or support vector machines and is illustrated as the red part in Figure 2. We further propose to construct a FGN using our small knowledgebase of genes and their phenotypic effects. Such a knowledgebase is indeed critical for any inference in FGN. Therefore, we propose to integrate protein-protein interactions, ND relevant interactions and microarray as well as SNP array data.

Starting from the gene groups we can identify their possible interaction partners, integrating the commercially available database Ingenuity www.ingenuity.com. The protein-protein (PPI) interactions for the extracted set of expressed genes can be derived from other freely available databases such as HPRD www.hprd.org, IntAct www.ebi.ac.uk/intact/, DIP dip.doe-mbi.ucla.edu/dip/ and many others. It is worth mentioning that after these extractions the resulting PPI is often filtered and only interactions supported by at least two lines of evidence are further considered. However, in the spirit of the FGN discussed above, we integrate all available interactions and leave it to the final investigator, which level of confidence he requires. Another feature of Ingenuity allows us to search diseases that have a relation to the candidate genes previously extracted. In our current study we restrict this search to ND and seek all genes related to these diseases. We exclude genes that show no relation to any of our candidates and keep the remaining to further grow our network. At this stage we can combine the two graphs generated from the two PPI approaches. Once the related ND are identified in Ingenuity we perform a literature search to extract microarray and SNP array experiments. Such datasets can for example be obtained by browsing the gene expression omnibus (GEO) from the website of the National Center for Biotechnology Information ncbi.nlm.nih.gov/geo/. In the last step we integrate these datasets and use them to refine the weights in the FGN, as briefly discussed above.

The final network is than thought to have comprehensive coverage due to the integration of genes, showing similar or equal function on the phenotypic level, the integration of direct interactions as obtained for PPI analysis and the integration of data from pathways related to ND – which is the focus of our study. Furthermore, it is thought to be reliable due to the integration of functional image features, microarray and SNP experiments. Additionally, further levels of knowledge can be integrated by literature searches.

The constructed network can now readily be used to infer genes that cause phenotypic variations similar to those from the knockdown experiments that lead to the initial neuronal images. This gives us a variety of discovery options. First, a network based in silica screen to identify genes that might cause the phenotypic changes of interest can be performed, using our image knowledge base. It is clear that any result has to be screened in a wetlab, but as discussed above a significantly lower number of experiments needs to be performed, leading to reduced costs and enhance efficiency. A particular interesting discovery would be a gene which causes the same dendritic spine phenotype, as inhibiting mTOR in ND. This gene would than either be involved upstream in the TSC-mTOR pathway or could be a potential downstream target. As mentioned earlier this pathway is connected to a variety of signals and its inhibition often leads to unexpected effects. Therefore, downstream targets of mTOR are of high interest. We mentioned that mTOR is the functional hub in the TSC-mTOR pathway and different clinical trials of mTOR inhibitors (mainly rapamycin analogues) are currently underway. However, the focus of these trails is on the treatment of cancers. A broader view on the role of the TSC-mTOR pathway in ND might therefore suggest possible therapeutical effects of mTOR inhibitors in these diseases.

V. Conclusions

We have described how a high-quality FGN can be inferred from high content screening data by integrating different data sources. In particular we propose to use dendritic spine image features, PPI, models of ND, gene and SNP expression profiles. The work presents a new angle on network construction which we call image based systems biology. It starts from an image and systematically integrates different data sources to assemble a probabilistic graph of gene functions. A main drawback of our approach is the accessibility and quality of neuronal images from different labs. We currently focus on the retrieval of image data, the construction of the network and more sophisticated techniques for data integration.

Acknowledgments

This work was supported in part by the NIH Grant R01 LM009161. Dominik Beck is partially supported by the UNSW IPRS scholarship.

References

1. Heitman J, Movva NR, Hall MN. Targets for cell cycle arrest by the immunosuppressant rapamycin in yeast. *Science*. 1991; 253:905–909. [PubMed: 1715094]
2. Huang J, Manning BD. The TSC1-TSC2 complex: a molecular switchboard controlling cell growth. *Biochem J*. June 1.2008 412:179–190. [PubMed: 18466115]
3. Guertin DA, Sabatini DM. Defining the Role of mTOR in Cancer. *Cancer Cell*. 2007; 12:9–22. [PubMed: 17613433]
4. Nobukuni T, Joaquin M, Roccio M, Dann SG, Kim SY, Gulati P, Byfield MP, Backer JM, Natt F, Bos JL, Zwartkruis FJT, Thomas G. Amino acids mediate mTOR/raptor signaling through activation of class 3 phosphatidylinositol 3OH-kinase. *Proceedings of the National Academy of Sciences of the United States of America*. 2005; 102:14238–14243. [PubMed: 16176982]
5. Sabatini DM. mTOR and cancer: insights into a complex relationship. *Nat Rev Cancer*. 2006; 6:729–734. [PubMed: 16915295]
6. Inoki K, Corradetti MN, Guan KL. Dysregulation of the TSC-mTOR pathway in human disease. *Nature Genetics*. 2005; 37:19–24. [PubMed: 15624019]
7. Hering H, Sheng M. Dendritic spines: Structure, dynamics and regulation. *Nature Reviews Neuroscience*. 2001; 2:880–888.
8. Sala C, Cambianica I, Rossi F. Molecular mechanisms of dendritic spine development and maintenance. *Acta Neurobiologiae Experimentalis*. 2008; 68:289–304. [PubMed: 18511962]
9. Goni J, Esteban F, de Mendizabal N, Sepulcre J, Ardanza-Trevijano S, Agirrezabal I, Villoslada P. A computational analysis of protein-protein interaction networks in neurodegenerative diseases. *BMC Systems Biology*. 2008; 2:52. [PubMed: 18570646]
10. Swiech L, Perycz M, Malik A, Jaworski J. Role of mTOR in physiology and pathology of the nervous system. *Biochimica et Biophysica Acta - Proteins and Proteomics*. 2008; 1784:116–132.
11. Bourne JN, Harris KM. Balancing structure and function at hippocampal dendritic spines. *Annual Review of Neuroscience*. 2008; 31:47–67.
12. Knobloch M, Mansuy IM. Dendritic spine loss and synaptic alterations in Alzheimer's disease. *Molecular Neurobiology*. 2008; 37:73–82. [PubMed: 18438727]
13. Gerfen CR. Indirect-pathway neurons lose their spines in Parkinson disease. *Nature Neuroscience*. 2006; 9:157–158.
14. Spires TL, Grote HE, Garry S, Cordery PM, Van Dellen A, Blakemore C, Hannan AJ. Dendritic spine pathology and deficits in experience-dependent dendritic plasticity in R6/1 Huntington's disease transgenic mice. *European Journal of Neuroscience*. 2004; 19:2799–2807. [PubMed: 15147313]

15. Kolluri N, Sun Z, Sampson AR, Lewis DA. Lamina-specific reductions in dendritic spine density in the prefrontal cortex of subjects with schizophrenia. *American Journal of Psychiatry*. 2005; 162:1200–1202. [PubMed: 15930070]
16. Hill JJ, Hashimoto T, Lewis DA. Molecular mechanisms contributing to dendritic spine alterations in the prefrontal cortex of subjects with schizophrenia. *Molecular Psychiatry*. 2006; 11:557–566. [PubMed: 16402129]
17. Glantz LA, Lewis DA. Decreased dendritic spine density on prefrontal cortical pyramidal neurons in schizophrenia. *Archives of General Psychiatry*. 2000; 57:65–73. [PubMed: 10632234]
18. Nimchinsky EA, Sabatini BL, Svoboda K. Structure and function of dendritic spines. *Annual Review of Physiology*. 2002; 64:313–353.
19. Kasai H, Matsuzaki M, Noguchi J, Yasumatsu N, Nakahara H. Structure-stability-function relationships of dendritic spines. *Trends in Neurosciences*. 2003; 26:360–368. [PubMed: 12850432]
20. Tavazoie SF, Alvarez VA, Ridenour DA, Kwiatkowski DJ, Sabatini BL. Regulation of neuronal morphology and function by the tumor suppressors Tsc1 and Tsc2. *Nat Neurosci*. 2005; 8:1727–1734. [PubMed: 16286931]
21. Cheng J, Zhou X, Sabatini BL, Wong STC. NeuronIQ: A novel computational approach for automatic dendrite spines detection and analysis. 2007 IEEE/NIH Life Science Systems and Applications Workshop, LISA. 2008:168–171.
22. Zhou X, Zhu J, Liu KY, Sabatini B, Wong S. Mutual information-based feature selection in studying perturbation of dendritic structure caused by TSC2 inactivation. *Neuroinformatics*. 2006; 4:81–94. [PubMed: 16595860]
23. Meikle L, Pollizzi K, Egnor A, Kramvis I, Lane H, Sahin M, Kwiatkowski DJ. Response of a Neuronal Model of Tuberous Sclerosis to Mammalian Target of Rapamycin (mTOR) Inhibitors: Effects on mTORC1 and Akt Signaling Lead to Improved Survival and Function. *J Neurosci*. May 21.2008 28:5422–5432. [PubMed: 18495876]
24. Biou V, Brinkhaus H, Malenka RC, Matus A. Interactions between drebrin and Ras regulate dendritic spine plasticity. *European Journal of Neuroscience*. 2008; 27:2847–2859. [PubMed: 18588530]
25. Calabrese B, Halpain S. Essential role for the PKC target MARCKS in maintaining dendritic spine morphology. *Neuron*. 2005; 48:77–90. [PubMed: 16202710]
26. Chen Y, Dube CM, Rice CJ, Baram TZ. Rapid loss of dendritic spines after stress involves derangement of spine dynamics by corticotropin-releasing hormone. *Journal of Neuroscience*. 2008; 28:2903–2911. [PubMed: 18337421]
27. Hongpaisan J, Alkon DL. A structural basis for enhancement of long-term associative memory in single dendritic spines regulated by PKC. *Proceedings of the National Academy of Sciences of the United States of America*. 2007; 104:19571–19576. [PubMed: 18073185]
28. Toliaas KF, Bikoff JB, Burette A, Paradis S, Harrar D, Tavazoie S, Weinberg RJ, Greenberg ME. The Rac1-GEF Tiam1 couples the NMDA receptor to the activity-dependent development of dendritic arbors and spines. *Neuron*. 2005; 45:525–538. [PubMed: 15721239]
29. Haeckel A, Ahuja R, Gundelfinger ED, Qualmann B, Kessels MM. The actin-binding protein Abp1 controls dendritic spine morphology and is important for spine head and synapse formation. *The Journal of neuroscience : the official journal of the Society for Neuroscience*. 2008; 28:10031–10044. [PubMed: 18829961]
30. Lee I, Lehner B, Crombie C, Wong W, Fraser AG, Marcotte EM. A single gene network accurately predicts phenotypic effects of gene perturbation in *Caenorhabditis elegans*. *Nature Genetics*. 2008; 40:181–188. [PubMed: 18223650]
31. Alexeyenko A, Tamas I, Liu G, Sonnhammer ELL. Automatic clustering of orthologs and inparalogs shared by multiple proteomes. *Bioinformatics*. 2006; 22:e9–e15. [PubMed: 16873526]
32. Jansen R, Yu H, Greenbaum D, Kluger Y, Krogan NJ, Chung S, Emili A, Snyder M, Greenblatt JF, Gerstein M. A Bayesian Networks Approach for Predicting Protein-Protein Interactions from Genomic Data. *Science*. 2003; 302:449–453. [PubMed: 14564010]
33. Lee I, Date SV, Adai AT, Marcotte EM. A probabilistic functional network of yeast genes. *Science*. 2004; 306:1555–1558. [PubMed: 15567862]

34. Lehner B, Lee I. Network-guided genetic screening: building, testing and using gene networks to predict gene function. *Brief Funct Genomic Proteomic*. April 29.2008 :eln020.
35. Huynen M, Snel B, Lathe W Iii, Bork P. Predicting protein function by genomic context: Quantitative evaluation and qualitative inferences. *Genome Research*. 2000; 10:1204–1210. [PubMed: 10958638]
36. Marcotte EM, Pellegrini M, Thompson MJ, Yeates TO, Eisenberg D. A combined algorithm for genome-wide prediction of protein function. *Nature*. 1999; 402:83–86. [PubMed: 10573421]
37. Jeong H, Mason SP, Baraba?si AL, Oltvai ZN. Lethality and centrality in protein networks. *Nature*. 2001; 411:41–42. [PubMed: 11333967]

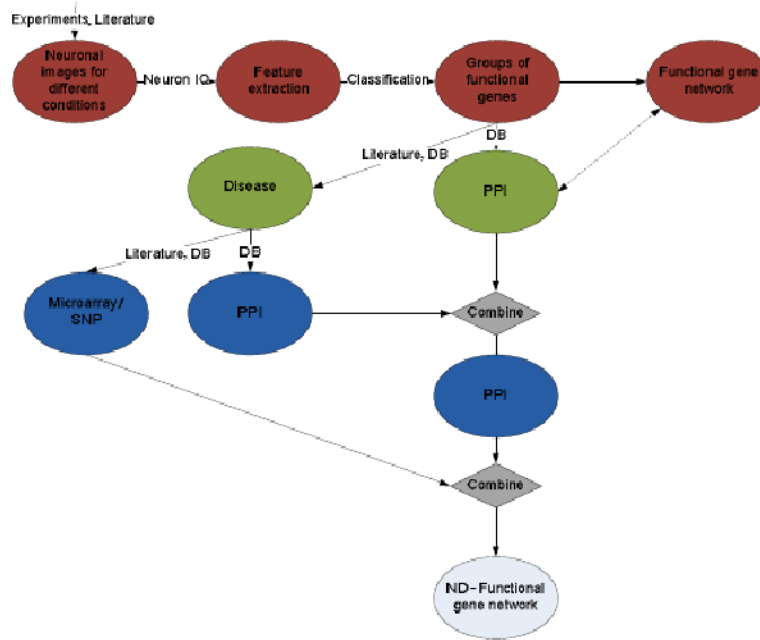


Fig. 2.
The graph illustrates the pipeline for the proposed network construction approach.

TABLE I

This table illustrates some experiments reporting changes of dendritic spine morphology. The conditions include knockouts, loss of function, overexpression (OE) and molecule exposure.

Gene	Condition	Influenced spine parameter	Reference
TSC2	RNAi	density, length	[20,22]
TSC2	RNAi + Rapamycin	density	[20,22]
TSC1	protein loss	density, length, head width	[20,22]
TSC1	loss + rapamycin	density, length	[23]
Drebrin	OE	shape	[24]
Drebrin	RNAi	size, shape	[24]
Ras	positive	shape	[24]
Ras	negative	no effect	[24]
MARCKS	RNAi	density, length, head width	[25]
MARCKS	OE	density, head width, length	[25]
NBI 30775	exposure	density	[26]
CRH	exposure	spine density	[26]
PKC	Bryostatin (activation)	density, shape	[27]
PKC	Ro 31-8220 (blocker)	density	[27]
TIAM1	RNAi	density, length, shape	[28]
TIAM1	OE	density	[28]
Abp1	OE	length, density	[29]
Abp1	RNAi	density	[29]